



---

**Delivery report**

PV-LAC: Advanced Land, Aerosol and Coastal products for PROBA-V

# **PV-LAC: D1-A2, Requirements Baseline Document Activity 2**

Yves Govaerts, Erwin Wolters, and Else Swinnen

May 2016



## Distribution List

### DISTRIBUTION LIST

Author(s) : Yves Govaerts, Erwin Wolters, and Else Swinnen

Reviewer(s) : Philippe Goryl, Fabrizio Niro

Approver(s) : Philippe Goryl, Fabrizio Niro

Issuing authority : VITO

## Change record

### CHANGE RECORD

Release	Date	Pages	Description of change	Editor(s)	Reviewer(s)
V1.0	30/04/2016	All	First version	Y. Govaerts, E. Wolters, E. Swinnen	Philippe Goryl, Fabrizio Niro
V1.1	20/05/2016	1	Adaptation GCOS requirements justified	Y. Govaerts	Else Swinnen, Philippe Goryl, Fabrizio Niro
		1	Added “per dedade” to “Stability” column heading	Y. Govaerts	
		2	Reformulation of text	Y. Govaerts	
		6	Equation number (1) and reference added	E. Wolters	
		6	Minor corrections to Eq. 1	E. Wolters	
		6	Various minor editorial modifications	E. Wolters	
		6	Included information on period of TOMS climatology	E. Wolters	
		7	Various clarifications, additions, and reformulations	E. Wolters	
		13	Additional statement on LUT interpolation	Y. Govaerts	
		17	Included information on satellite spatial resolution corresponding to surface observation averaging time	E. Wolters	
		18	Various clarifications on validation approach	E. Wolters	
		18	Figure with global distribution of selected AERONET and CEOS PICS sites included	E. Wolters	
		18	Validation approach modified and further clarified.	E. Wolters	
		19	Text on validation metrics moved to separate subsection	E. Wolters	

## TABLE OF CONTENTS

<b>Distribution List</b>	<b>i</b>
<b>Change record</b>	<b>ii</b>
<b>Table of Contents</b>	<b>iii</b>
<b>List of Figures</b>	<b>v</b>
<b>List of Tables</b>	<b>vi</b>
<b>List of Abbreviations and Acronyms</b>	<b>vii</b>
<b>CHAPTER 1 Introduction</b>	<b>1</b>
<b>CHAPTER 2 Physics of the signal</b>	<b>2</b>
<b>CHAPTER 3 Current PROBA-V Atmospheric Correction method</b>	<b>6</b>
<b>CHAPTER 4 Analysis of existing approaches</b>	<b>9</b>
4.1. <i>Criteria for retrieval method evaluations</i>	9
4.2. <i>Identification of existing approaches</i>	9
4.3. <i>Forward Radiative Transfer</i>	11
4.3.1. Surface reflectance (SRE)	11
4.3.2. Surface-atmosphere radiative coupling (SAC)	11
4.3.3. Aerosols	12
4.4. <i>Inversion method</i>	13
4.4.1. RTM solving	13
4.4.2. Prior information (PRI)	13
4.4.3. Multi-dimensional retrieval (DIM)	14
4.5. <i>Discussion</i>	14
<b>CHAPTER 5 Atmospheric Correction Validation</b>	<b>15</b>
5.1. <i>Aerosol Optical Thickness and atmospheric correction validation</i>	15
5.2. <i>State-of-the-art on Atmospheric Correction validation</i>	15
5.2.1. AOT retrieval validation	15
5.2.2. Surface reflectance validation	16
5.3. <i>Comparison of satellite with ground-based observations</i>	17
5.4. <i>Validation approach</i>	17
5.4.1. Aerosol Optical Thickness validation	18
5.4.2. TOC reflectance validation	18

Table of Contents

5.4.3. validation metrics \_\_\_\_\_ 19

**Literature** \_\_\_\_\_ **20**

## LIST OF FIGURES

Figure 1: Simulated near-surface BRF in the principal plane for the PROBA-V BLUE (top panel) and RED (bottom panel) bands over vegetated surface with LAI = 3 calculated with the model of N. Gobron et al., 1996. The green line shows the TOC or surface reflectance in absence of any atmospheric effect. The red (blue) lines show the apparent surface or bottom of atmosphere (BOA) reflectance for an aerosol optical thickness at 0.55 $\mu\text{m}$ of 0.2 (0.6).....	3
Figure 2: Surface reflectance and Top of Atmosphere (TOA) reflectance in the principle plane for all PROBA-V spectral bands for an aerosol optical thickness of 0.2 and 0.6 at 0.55 $\mu\text{m}$ .....	5
Figure 3: Global distribution of selected AERONET and CEOS PICS sites.....	18

## LIST OF TABLES

Table 1: GCOS requirements for surface albedo ECV generation (Systematic Observation Requirements for Satellite-Based Data Products for Climate, 2011 Update) .....	1
Table 2: Rayleigh and aerosol optical thicknesses in the PROBA-V spectral bands for the cases simulated on Figure 1 and Figure 2. ....	2
Table 3: Typical total gaseous transmittance in the PROBA-V bands for a standard midlatitude summer atmosphere (Anderson et al., 1986) with a total water vapour column of $28.86 \text{ kg m}^{-2}$ and a total ozone column of 335.31 Dobson Units (DU).....	2
Table 4: List of assumptions on the forward RTM and numerical methods for retrieving surface reflectance from satellite observations.....	9
Table 5: List of reviewed key publications with the associated assumption described in Table 4. ...	10



## LIST OF ABBREVIATIONS AND ACRONYMS

AER	Aerosols
AERONET	Aerosol Robotic Network
AOT	Aerosol Optical Thickness
BOA	Bottom of Atmosphere
BHR	Bidirectional Hemispherical Reflectance
BRF	Bidirectional Reflectance Factor
CALIOP	Cloud-Aerosol Lidar with Orthogonal Polarization
CEOS PICS	Committee on Earth Observation Satellites Pseudo Invariant Calibration Sites
DHR	Directional Hemispherical Reflectance (black sky)
DIM	Multi-Dimensional Retrieval
DU	Dobson Units
ECMWF	European Centre for Mid-Range Weather Forecasts
ECV	Essential Climate Variable
ESA	European Space Agency
EUMETSAT	European Organisation for the Exploitation of Meteorological Satellites
FCI	Flexible Combined Imager
FLUXNET	Flux Tower Network
GCOS	Global Climate Observing System
GEO	Geosynchronous Equatorial Orbit
GOES	Geostationary Operational Environmental Satellite
GOME	Global Ozone Monitoring Experiment
JMA	Japanese Meteorological Agency
LEO	Low Earth Orbit
LER	Lambertian Equivalent Reflectance
LUT	Look-Up Table
MISR	Multi-Angle Imaging Spectroradiometer
MODIS	Moderate-Resolution Imaging Spectroradiometer
MSG	Meteosat Second Generation
MTG	Meteosat Third Generation
NDVI	Normalized Difference Vegetation Index
NIR	Near Infrared
NWP	Numerical Weather Prediction Model

## List of Abbreviations and Acronyms

NOAA	National Oceanic and Atmospheric Administration
OE	Optimal Estimation
OMI	Ozone Monitoring Instrument
POLDER	Polarization and Directionality of the Earth's Reflectances
PRI	Prior Information
PROBA-V	Project for On-Board Autonomy – Vegetation
PV-LAC	Advanced Land, Aerosol, and Coastal Products for PROBA-V
RTLS	Ross-Thick Li-Sparse
RTM	Radiative Transfer Model
6S	Second Simulation of the Satellite Signal in the Solar Spectrum
SAC	Surface-Atmosphere Coupling
SCIAMACHY	Scanning Imaging Absorption Spectrometer for Atmospheric Chartography
SMAC	Simple Model for Atmospheric Correction
SPOT-VEGETATION	Satellite Pour l'Observation de la Terre - Végétation
SOL	Radiative Transfer Model Solving
SRE	Surface Reflectance
RTM	Radiative Transfer Model
SEVIRI	Spinning Enhanced Visible and Infrared Imager
TOA	Top Of Atmosphere
TOC	Top of Canopy
TN	Technical Note
TOMS	Total Ozone Mapping Spectrometer
UV	Ultra Violet
VIS	Visible

## CHAPTER 1 INTRODUCTION

This document establishes the requirements for surface reflectance generation from PROBA-V observations and the associated retrieval method to achieve these requirements. These requirements are taken from Global Climate Observation System (GCOS) surface albedo generation (see Table 1).

These requirements have been established for the generation of surface albedo Essential Climate Variables (ECVs). The objective behind these numbers is to detect 20% of the expected total change in radiative forcing per decade resulting from greenhouse gases and other atmospheric constituents, i.e.,  $\sim 0.1 \text{ W m}^{-2}$  per decade. These requirements are global and concern the generation of climate data records, but cannot be straightforwardly converted into requirements to support near-real time operational applications, such as agriculture monitoring. As this work focuses on the possibility to generate a surface ECV, GCOS requirements are currently used.

*Table 1: GCOS requirements for surface albedo ECV generation (Systematic Observation Requirements for Satellite-Based Data Products for Climate, 2011 Update)*

Variable/ Parameter	Horizontal Resolution	Temporal Resolution	Accuracy	Stability per decade
DHR	1 km	Daily to weekly	max(5%; 0.0025)	max(1%; 0.0001)
BHR <sub>iso</sub>	1 km	Daily to weekly	max(5%; 0.0025)	max(1%; 0.0001)

In order to discuss the possibility to meet these requirements, existing approaches for the surface reflectance retrieval from space observations, i.e., corrected for atmospheric effects, have been reviewed. This analysis is performed in the light of the physics of the signal observed by PROBA-V, the retrieval constraints, and the mission objectives, i.e., the requested surface BRF accuracy to perform atmospheric correction over land surfaces. The objective is to determine which approach and associated assumptions are most appropriate for the surface reflectance and aerosol properties retrieval from PROBA-V observations. To this end, the radiative processes determining the PROBA-V observations, and in particular the radiative interactions between the surface and the atmosphere are described in CHAPTER 2. A description of the current PROBA-V atmospheric correction method is given in CHAPTER 3. Criteria for the evaluation are established in Section 4.1, while the reviewed methods are listed in Section 4.2. These approaches are analysed in terms of the forward radiative transfer model (Section 4.3) and numerical inversion methods (Section 4.4). The choice for the proposed method in the framework of this study is discussed in Section 4.5. A literature review on the AOT and atmospheric correction validation, as well as a proposed validation approach of these parameters within this project is given in CHAPTER 5.

## CHAPTER 2    PHYSICS OF THE SIGNAL

Fundamentally, the spectral radiance derived from a satellite measurement in the solar spectrum is controlled by all interactions through the various atmospheric parts and the underlying surface. Hence, the elaboration of surface reflectance maps from PROBA-V observations requires addressing a series of technical and physical issues. Among the physical issues, the radiative coupling between aerosols and surface scattering is certainly one of the most challenging problems to be solved. Indeed, aerosols contribute to sky radiation modifying thereby the amount of radiation reflected by the surface as a function of wavelength and viewing directions.

*Table 2: Rayleigh and aerosol optical thicknesses in the PROBA-V spectral bands for the cases simulated on Figure 1 and Figure 2.*

Optical Thickness	Blue	Red	NIR	SWIR
Rayleigh	0.194	0.048	0.018	0.001
Aerosol (thin)	0.263	0.149	0.094	0.025
Aerosol (thick)	0.789	0.447	0.282	0.076

*Table 3: Typical total gaseous transmittance in the PROBA-V bands for a standard midlatitude summer atmosphere (Anderson et al., 1986) with a total water vapour column of 28.86 kg m<sup>-2</sup> and a total ozone column of 335.31 Dobson Units (DU).*

BAND	TOTAL	H <sub>2</sub> O	O <sub>3</sub>	O <sub>2</sub>	CO <sub>2</sub>
BLUE	<b>0.993</b>	1.000	0.997	1.000	1.000
RED	<b>0.959</b>	0.990	<b>0.979</b>	<b>0.989</b>	1.000
NIR	<b>0.926</b>	<b>0.929</b>	0.999	0.998	1.000
SWIR	<b>0.974</b>	0.994	1.000	1.000	<b>0.981</b>

The discrimination between the signal reflected by the surface from the one scattered by aerosols represents one of the major issues when retrieving surface Bi-directional Reflectance Factor (BRF) from space observations. This problem is further complicated by the intrinsic anisotropic radiative behaviour of natural surfaces and its strong coupling with atmospheric radiative processes. In case of PROBA-V, the presence of water absorption bands in several spectral bands adds a level of complexity to this retrieval. These effects are illustrated on Figure 1 and Figure 2. An increase in atmospheric aerosol concentration (see Table 2) is responsible for an increase of solar radiation scattered by the atmosphere, *i.e.*, the fraction of diffuse sky radiation which, in turn, smoothes the effects of surface anisotropy, particularly in the BLUE and RED spectral bands (Figure 1). This smoothing effect decreases with wavelength as the corresponding aerosol optical thickness decreases. In the SWIR band, scattering processes in the atmosphere are negligible and the major contribution of the atmosphere is absorption by CO<sub>2</sub> and H<sub>2</sub>O.

Therefore these examples show that the accuracy with which it is possible to retrieve surface reflectance is closely controlled by the knowledge of the atmospheric aerosol amount that shapes the surface BRF.

This smoothing effect impacts the surface albedo. Typically, the difference in the surface albedo (Directional Hemispherical Reflectance, DHR) calculated with actual surface reflectance (green curves in Figure 1 and Figure 2) or the apparent one (red/light blue curves) is in the range of  $\pm 2\%$ . Such an error is not in agreement with the GCOS stability requirements (see Table 1).

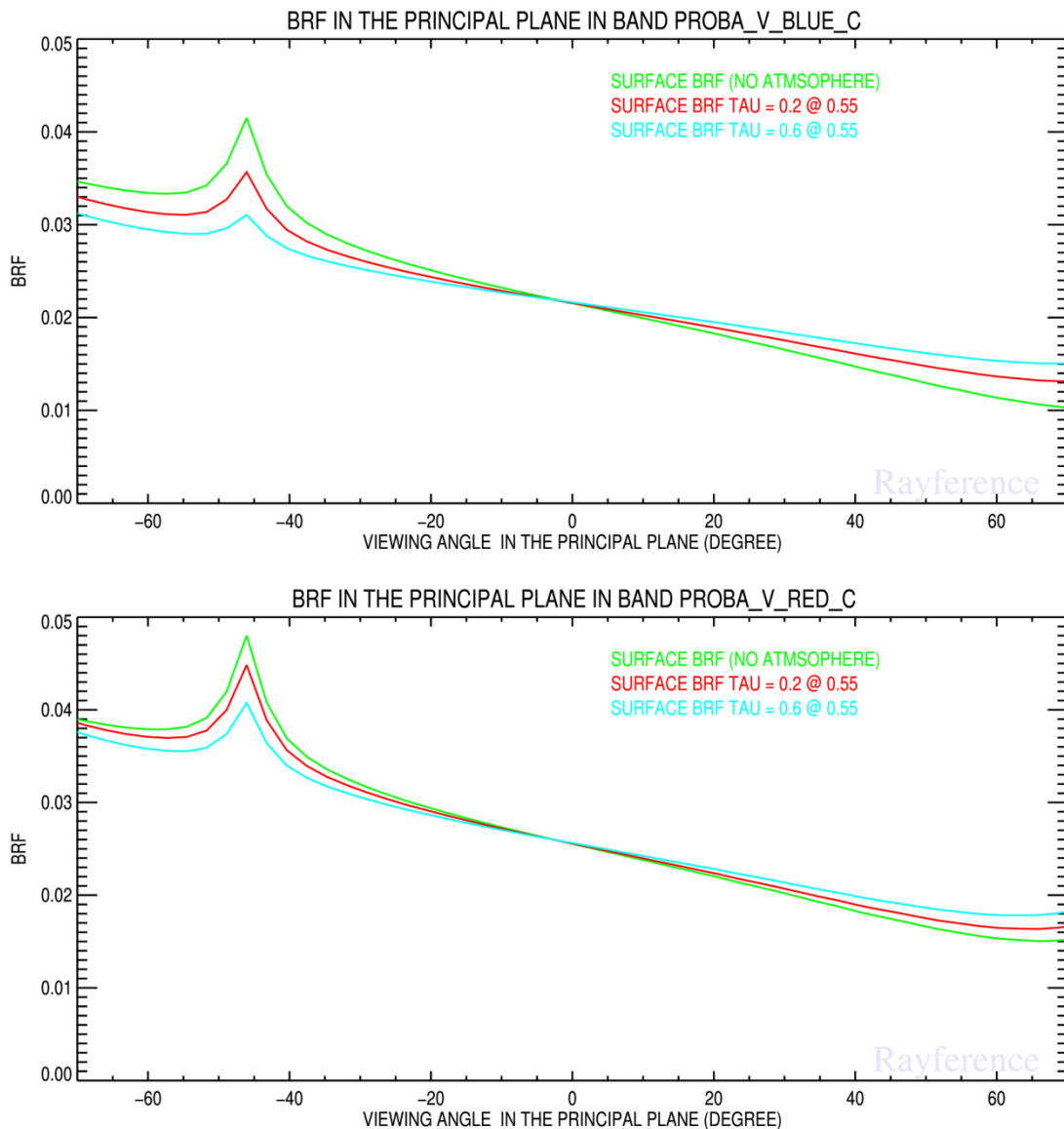
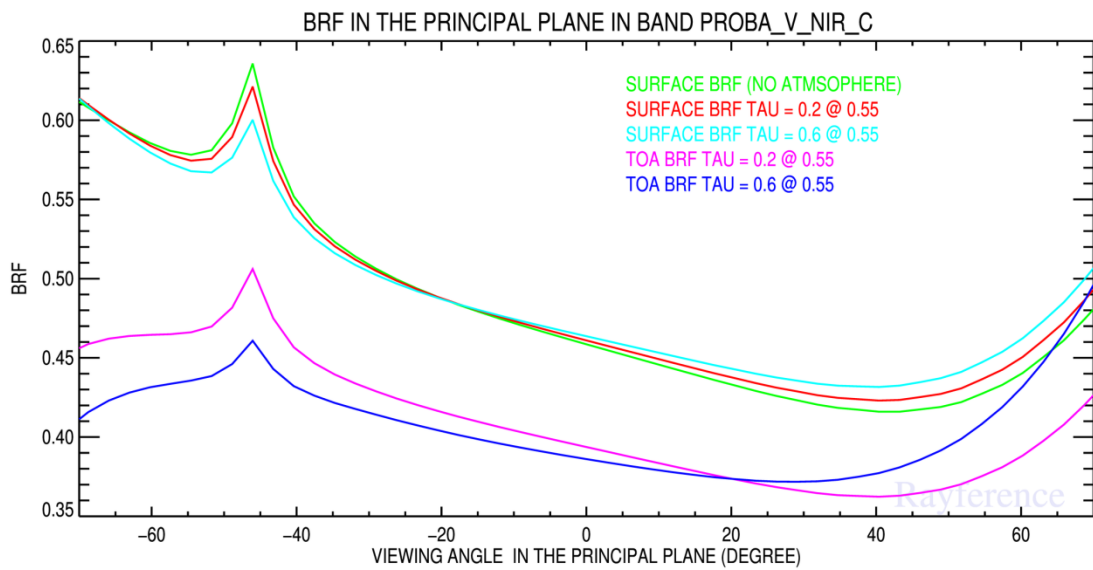
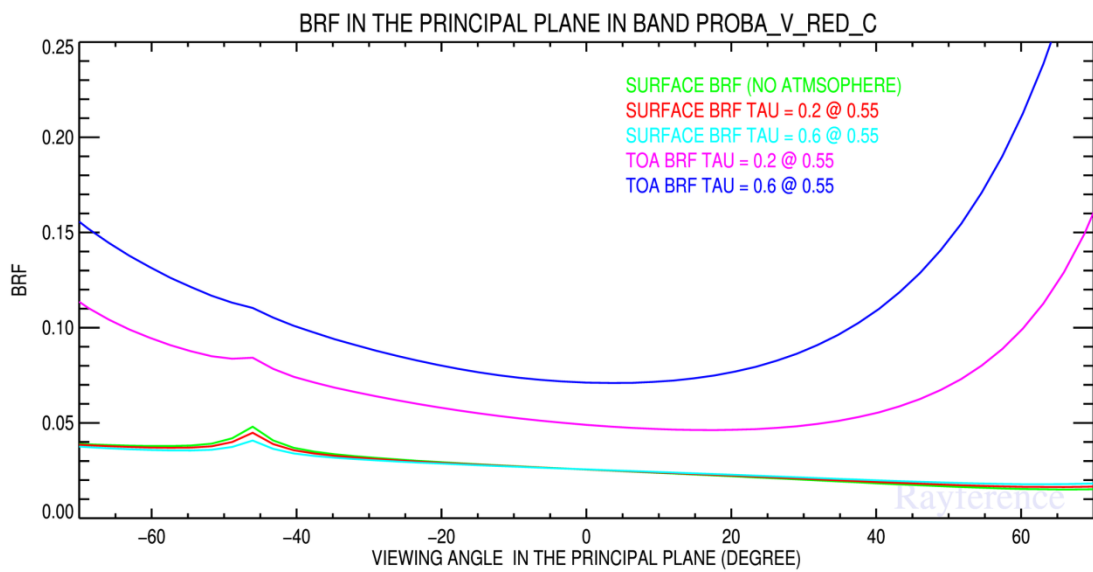
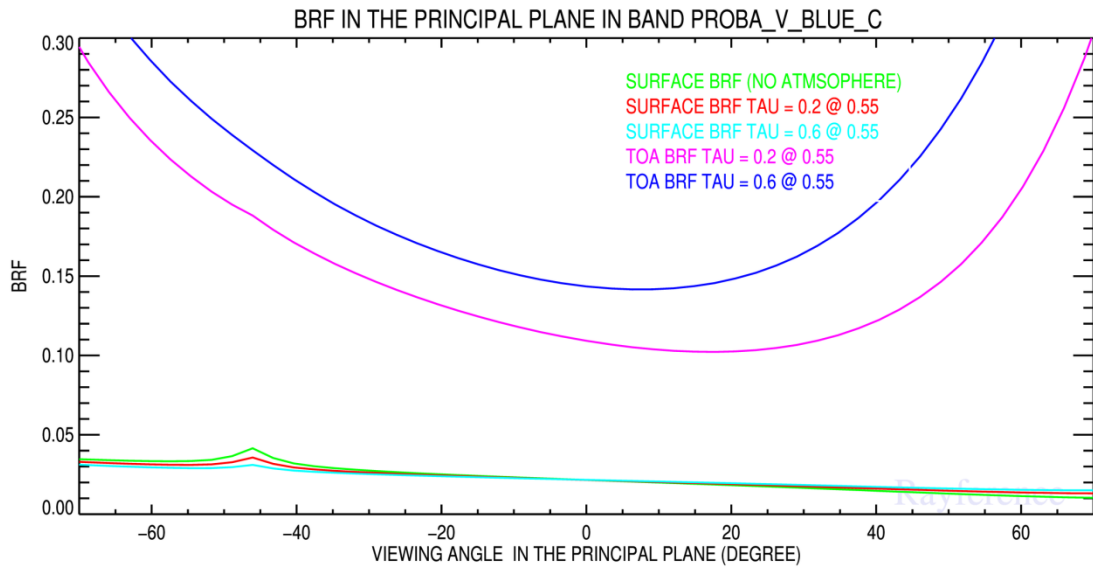


Figure 1: Simulated near-surface BRF in the principal plane for the PROBA-V BLUE (top panel) and RED (bottom panel) bands over vegetated surface with LAI = 3 calculated with the model of N. Gobron et al., 1996. The green line shows the TOC or surface reflectance in absence of any atmospheric effect. The red (blue) lines show the apparent surface or bottom of atmosphere (BOA) reflectance for an aerosol optical thickness at 0.55  $\mu\text{m}$  of 0.2 (0.6).

# Physics of the signal



Physics of the signal

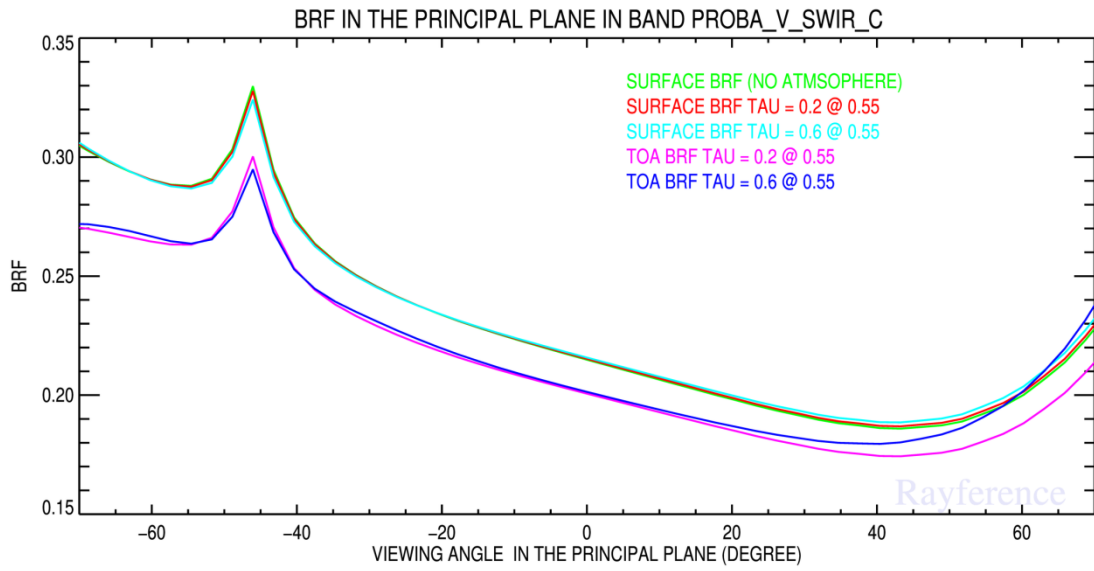


Figure 2: Surface reflectance and Top of Atmosphere (TOA) reflectance in the principle plane for all PROBA-V spectral bands for an aerosol optical thickness of 0.2 and 0.6 at 0.55  $\mu\text{m}$ .

## CHAPTER 3 CURRENT PROBA-V ATMOSPHERIC CORRECTION METHOD

The current PROBA-V atmospheric correction procedure, which includes an aerosol optical thickness retrieval, is based on an implementation of the Simple Model for Atmospheric Correction, (SMAC, [Raman and Dedieu, 1994]). SMAC converts the observed TOA into TOC reflectance taking into account molecular and aerosol scattering, thereby using auxiliary input data, such as water vapour, ozone, and surface pressure to account for the atmospheric extinction.

SMAC estimates the TOC reflectance using the available knowledge on the atmospheric constituents (water vapour, ozone, aerosols, etc.) and altitude. The scattering and absorption processes within the atmospheric column are parameterised by analytical formulations, whose coefficients are spectrally dependent and which are fitted against Second Simulation of the Satellite Signal in the Solar Spectrum (6S, Vermote et al., 1997) reference code. The 6S radiative transfer model includes multiple aerosol types, such as continental, stratospheric, and desertic.

The TOC reflectance can be described as a function of the TOA reflectance as follows (Eq. 1):

$$R_{TOC}(\theta_s, \theta_v, \Delta\varphi) = \frac{R_{TOA}(\theta_s, \theta_v, \Delta\varphi) - T_{gas}(\theta_s, \theta_v) R_{atm}(\theta_s, \theta_v, \Delta\varphi)}{T_{gas}(\theta_s, \theta_v) T_{tot}(\theta_v) + [R_{TOA}(\theta_s, \theta_v, \Delta\varphi) - T_{gas}(\theta_s, \theta_v) R_{atm}(\theta_s, \theta_v, \Delta\varphi)] s} \quad , Eq. (1)$$

in which  $R_{TOA}$  is the Top-of-Atmosphere reflectance,  $\theta_s$  the solar zenith angle,  $\theta_v$  the viewing zenith angle,  $\Delta\varphi$  the relative azimuth angle,  $T_{gas}$  the total (two-way) gaseous transmission,  $R_{atm}$  the atmospheric reflectance,  $T_{tot}$  the total atmospheric diffuse transmittance, and  $s'$  the atmosphere's spherical albedo.

The above equation monochromatically calculates the TOC reflectance. To obtain convoluted TOC reflectances, the underlying 6S code integrates each term in 2.5 nm steps over the respective spectral interval and finally derives  $R_{TOC}$ . See Vermote et al. (1997) and Rahman and Dedieu (1994) for a full set of equations and accompanying elaborations.

The auxiliary data that are ingested in SMAC are the following:

- Water vapour
- Ozone
- Surface pressure
- Tropospheric and stratospheric aerosol information

The water vapour information to estimate the column-integrated absorption is retrieved from ECMWF NWP data, delivered by MeteoServices. For each PROBA-V observation, water vapour data from four model runs per day (at 0, 6, 12, and 18 UTC) are used and are interpolated linearly in time between the two closest observation and bilinear in space.

Information on the atmospheric ozone concentration is derived from monthly climatology maps based on 11 years of Total Ozone Mapping Spectrometer (TOMS) observations prepared by the Centre d'Études Spatiales de la Biosphère (CESBIO, Berthelot and Dedieu, 1997).



## Current PROBA-V Atmospheric Correction method

Surface pressure information is obtained from the Global Land Surface Digital Elevation Model (GLSDEM), with the conversion from height to pressure calculated using an approach by Plummer et al. (2003):

$$P_{atm} = 1013.25 \left(1 - \frac{0.0065h}{288.16}\right)^{5.31}$$

This formula is a simplification of the barometric pressure equation, in which atmospheric pressure is related to elevation  $h$ , accounting for the lapse rate (decrease of temperature with height), the specific gas constant, and the air molar mass. The GLSDEM data have a horizontal resolution of ~90 m and a latitudinal extent from 56°S – 86°N.

The aerosol optical thickness (AOT) calculation is based on a method of Maisongrande et al. (2001), which was initially applied to SPOT-VEGETATION reflectance observations and which utilises a relation between NDVI at TOA and the observed SWIR reflectance. This AOT retrieval is performed as follows:

1. For each spectral channel, an initial atmospheric correction is calculated taking only gaseous absorption by water vapour and ozone and molecular scattering into account. This initial atmospheric correction is only applied to pixels that are labeled as 'clear' by the preceding cloud screening algorithm and further not labeled as 'snow/ice'. The obtained reflectances are hereafter referred to as  $R_{TOC,mol}$ .
2. From the  $NIR_{TOA}$  and  $RED_{TOA}$  reflectances, the  $NDVI_{TOA}$  is calculated.
3. From the  $NDVI_{TOA}$ ,  $Ratio = R_{SWIR,TOC} / R_{BLUE,TOC}$  is derived, using the relation  $Ratio = 1.305 * \exp(3.225 * NDVI_{TOA})$ . This also gives information on  $R_{SWIR,TOC}$ , because in the SWIR spectral range the atmospheric scattering is negligible and thus  $R_{SWIR,TOC} = R_{SWIR,mol}$ .
4.  $R_{BLUE,TOC}$  is calculated from  $Ratio$  and  $R_{SWIR,TOC}$  obtained in the previous step.
5. For aerosol optical thickness values of 0.05, 0.15, 0.30, and 0.50, the difference between reflectance from SMAC with full atmospheric correction (gaseous absorption + molecular scattering + aerosol contribution) and  $R_{BLUE,TOC}$  obtained in step 4 is calculated. The retrieved aerosol optical thickness is one of the four AOT values above for which this difference is minimal.
6.  $NDVI_{TOC,mol}$  and  $R_{SWIR,TOC,mol}$  are assessed against thresholds of  $> 0.2$  and  $< 0.4$ , respectively. For pixels fulfilling these criteria, the aerosol optical thickness follows from the retrieved value in step 5. For pixels outside these criteria, the aerosol optical thickness is empirically estimated based on the latitude of observation:

$$AOT_{0.55} = 0.2(\cos(\varphi) - 0.25)\sin(\varphi + \frac{\pi}{2})^3 + 0.05,$$

in which  $\varphi$  represents the latitude in radians.

7. Subsequently, the obtained AOT representative at 0.55  $\mu\text{m}$  is converted to corresponding BLUE, RED, NIR, and SWIR values using a continental aerosol model and full atmospheric corrections to all TOA reflectances are performed.

The above methodology is applied with the following restrictions:

## Current PROBA-V Atmospheric Correction method

- The aerosol optical thickness retrieval and subsequent atmospheric correction is performed for each 8<sup>th</sup> pixel in both across and along track directions. The remaining pixel values in the 8 × 8 box are obtained using bilinear interpolation.
- The coefficients in *Ratio* were adopted from the SPOT-VEGETATION values, which implies that spectral differences between the corresponding PROBA-V and SPOT-VEGETATION channels, however small, were not taken into account. Furthermore, this empiric relation is subject to seasonal and regional changes.

## CHAPTER 4 ANALYSIS OF EXISTING APPROACHES

---

### 4.1. CRITERIA FOR RETRIEVAL METHOD EVALUATIONS

The analysis of existing approaches for the retrieval of surface reflectance from space observations is based on two major criteria: (i) the series of assumptions concerning the underlying radiative processes, *i.e.*, the forward radiative transfer model (RTM) and (ii) the numerical method for solving the radiative transfer problem. This review is performed keeping in mind the type of observations acquired by PROBA-V and the requirements on the surface bi-directional factor (BRF) retrieval accuracy, including its impact on the diurnal cycle retrieval. Concerning the forward RTM, the following aspects are relevant:

- *Surface reflectance (SRE).*
- *Surface-atmosphere radiative coupling (SAC).*
- *Atmospheric correction (AER).*

Concerning the numerical method for the forward model inversion against observations, the following points are important:

- *RTM solving (SOL).*
- *Prior information (PRI).*
- *Multi-dimensional inversion (DIM).*

These assumptions are described in Table 4.

### 4.2. IDENTIFICATION OF EXISTING APPROACHES

Table 5 summarizes a publication list analysed in the framework of this Baseline Requirement Document, according to the assumptions described in Table 4. Assumptions that are not acceptable to fulfil the requirements are indicated in red, otherwise in green. Those that are acceptable under certain circumstances are indicated in yellow, as discussed in the next Sections. The current PROBA-V atmospheric correction method is referred to in Table 5 as 'Rahman and Dedieu (1994)/Sterckx et al. (2014)'.

*Table 4: List of assumptions on the forward RTM and numerical methods for retrieving surface reflectance from satellite observations.*

Topic	Type	Description
SRE	ISO	Forward RTM assumes Lambertian surface reflectance.
	ANI	Forward RTM assumes anisotropic surface BRF.
SAC	LER	Surface-atmospheric radiative coupling is based on the Lambertian equivalent reflectance assumption.
	ASC	Surface-atmospheric radiative coupling assumes anisotropic surface BRF and its proper coupling with aerosol multiple scattering.

## Analysis of existing approaches

<b>AER</b>	MIN	Atmospheric correction is based on the assumption that aerosol atmospheric scattering increases the top-of-atmosphere (TOA) BRF.
	PRE	Prescribed aerosol type and amount is used for the atmospheric correction.
	JOI	Aerosol amount and/or type are jointly retrieved with the surface reflectance.
<b>SOL</b>	EMP	There is no explicit RTM solution. Only an empirical approach is used.
	LUT	The forward RTM is solved with pre-computed LUTs.
	EXP	The forward model is explicitly solved allowing for a continuous variation of the state variables in the solution space.
<b>PRI</b>	NO	The mathematical processing of the prior information and assumptions are not taken into account in the solution cost estimation.
	OE	The mathematical processing of the prior information and assumptions are taken into account in the solution cost estimation.
<b>DIM</b>	A	Angular dimension
	S	Spectral dimension
	X	Spatial dimension
	T	Temporal dimension

Table 5: List of reviewed key publications with the associated assumption described in Table 4.

Reference	Orbit	SRE	SAC	AER	SOL	PRI	DIM
Bernard et al. (2011)	GEO	ISO	LER	MIN	LUT	NO	T
Dubovik et al. (2011)	GEO/LEO	ANI	ASC	JOI	EXP	OE	ASXT
Geiger et al. (2008)	GEO	ANI	LER	PRE	EXP	OE	A
Govaerts and Lattanzio (2007)	GEO	ANI	ASC	JOI	LUT	NO	A
Govaerts et al. (2010)	GEO	ANI	ASC	JOI	LUT	OE	AS
Herman and Celarier (1997)	LEO	ISO	LER	MIN	EMP	NO	T
Jin et al. (2003)	LEO	ANI	LER	PRE	EXP	NO	A
Kleipool et al. (2008)	LEO	ISO	LER	MIN	LUT	NO	T
Knapp et al. (2005)	GEO	ISO	LER	MIN	LUT	NO	T
Koelemeijer et al. (2003)	LEO	ISO	LER	MIN	LUT	NO	T
Martonchik (1997)	LEO	ANI	ASC	JOI	LUT	NO	A
Rahman and Dedieu (1994)/Sterckx et al. (2014)	LEO	ISO	LER	PRE	EMP	NO	
Vermote and Vermeulen (1999)	LEO	ISO	LER	PRE	LUT	NO	
Vermote et al. (2009)	LEO	ANI	ASC	PRE	LUT	NO	A

### 4.3. FORWARD RADIATIVE TRANSFER

#### 4.3.1. SURFACE REFLECTANCE (SRE)

Figure 1 and Figure 2 show examples of typical surface anisotropy in the PROBA-V spectral bands over uniformly vegetated surfaces. The illustrated smoothing effects increase as the wavelength decreases, so that the surface BRF cannot be neglected. The proposed retrieval method for surface reflectance should be able to deliver such information at any processed wavelength.

*However, that does not prevent to use a forward method that assumes a Lambertian surface as proposed by Vermote et al. (2002) and subsequently assemble observations acquired at different viewing/illumination geometries to derive the surface BRF (Jin et al. 2003). Hence, none of the listed approaches in Table 5 is likely to be rejected, because of the ISO assumption at this stage. However, such an assumption introduces uncertainties, as will be explained in Section 4.3.2.*

#### 4.3.2. SURFACE-ATMOSPHERE RADIATIVE COUPLING (SAC)

Atmospheric correction assuming Lambertian reflectance greatly simplifies the radiative transfer modelling, making the operational algorithm faster when the RTM inversion is based on pre-computed Look-Up-Tables (LUT). On the other hand, uncompensated atmospheric scattering caused by Lambertian models systematically biases the results (Wang et al. 2010). These authors have shown that the magnitude of biases grows with the amount of scattering in the atmosphere, *i.e.*, at shorter wavelengths and higher aerosol concentrations. The Lambertian assumption<sup>1</sup> redistributes reflected radiation over all directions, reducing reflectance where the BRF is high and enhancing it where the BRF is low (*e.g.*, Lyapustin 1999; Vermote and Vermeulen 1999). For a typical bowl-shaped BRF, this assumption will produce higher reflectance for near-nadir view and lower reflectance at high viewing/solar zenith angles. The error increases with the amount of total scattering in the atmosphere, in other words, at shorter wavelengths and at higher aerosol optical thickness. The bias can be very large in the angular regions of high BRF anisotropy, for example in the broad glint region and in the backscattering region over snow-covered surfaces (Lyapustin et al. 2009).

---

<sup>1</sup> In this case the LER assumption is used in inverse and not forward modelling. Hence, the question whether to use the BRF or DHR values is irrelevant.

## Analysis of existing approaches

In case of the MODIS algorithm, these atmospherically corrected surface reflectances are subsequently accumulated over a 16-day period to retrieve parameters of the Ross-Thick Li-Sparse (RTLS) BRF model (Lucht, Schaaf, and Strahler 2000) and to obtain surface albedo. Inherently, the surface reflectance biases are translated into a reduced anisotropy of the RTLS model, which may also affect albedo, as revealed by several large-scale investigations of the MODIS surface reflectance. These analyses demonstrated an underestimation of the MODIS surface reflectance in the visible bands, especially at large view angles (*e.g.*, Pinty et al. 2011). The Lambertian assumption certainly plays a role in this bias (Wang et al. 2010).

*Hence, methods listed in Table 5 that rely on the Lambertian assumption are not adequate for an accurate surface reflectance retrieval. Such a constraint also means that the RTM should be able to represent non-Lambertian surfaces, so that the ISO assumption is not acceptable. Similarly, Vermote et al. (2009) propose an improved algorithm for the retrieval of MODIS surface reflectance based on the inversion of 16-days accumulated MODIS observations in order to account for the surface anisotropy.*

### 4.3.3. AEROSOLS

Figure 1 and Figure 2 illustrate how the amount of diffuse atmospheric radiation, which varies as a function of wavelength and aerosols amount, shapes the surface BRF. Additionally, atmospheric aerosol scattering can affect the magnitude of the TOA BRF. Therefore it is necessary to correctly account for aerosol effects in the surface reflectance retrieval. Most of the reviewed methods in Table 5 assume that aerosols tend to increase surface reflectance, so that the selection of the darkest or so observations of a time series tends to be aerosol-free. Such a MIN assumption suffers from several limitations. First, aerosols increase the TOA BRF when their single scattering albedo (SSA) is close to 1 (so only slight absorption) and the magnitude of the BRF does not exceed 0.15-0.2, which typically occurs over snow-free vegetated surfaces at wavelengths shorter than 0.60  $\mu\text{m}$ . Other methods use prescribed aerosol type and amount (PRE).

Cases illustrated in Figure 1 and Figure 2 show the tight radiative coupling between aerosol scattering and surface BRF. Therefore it is important that the forward RTM properly accounts for these effects. However, in order to secure the accuracy or the possibility to increase the retrieval accuracy if needed, accounting for this coupling over non-Lambertian surfaces tremendously complicates the inversion process. It is recommended to select a method that does offer this option. Only a very limited number of methods offer such a possibility. When prescribed (PRE) aerosol models and amount are used for the atmospheric correction, it is critical that the correct phase function is used, otherwise it will not be possible to retrieve the surface anisotropy correctly.

Pinty et al. (2000) pioneered in the development of methods for the joint retrieval of surface BRF and aerosol load. In order to speed up the forward RTM, all solutions are pre-computed in LUTs for a limited number of surface parameter values and aerosol loads. No LUT entry interpolation is performed to further speed-up the retrieval process. This method has been improved to include an estimation of the retrieval error (Govaerts and Lattanzio 2007), which accounts for the actual radiometric performance of any processed geostationary instrument. In their approach, assumptions such as the aerosol amount invariance during the course of the day are converted into equivalent radiometric errors. This approach has been used to process all geostationary observations archived by the European Organisation for the Exploitation of Meteorological Satellites (EUMETSAT), the National Oceanic and Atmospheric Agency (NOAA), and the Japanese Meteorological Agency (JMA) (Govaerts et al. 2008). It has been subsequently improved by Govaerts et al. (2010) who introduced different aerosol models including non-spherical particles and a proper mathematical handling of the prior information in the framework of optimal

## Analysis of existing approaches

estimation (OE, Rodgers 2000) for processing MSG/SEVIRI observations. However, it still suffers from several drawbacks:

- The forward RTM is pre-computed and stored in LUTs, which limits the state variable space boundaries and the forward RTM accuracy, except when interpolation between the LUT nodes is performed, which is very CPU-demanding. To speed-up processing time, no interpolation is performed between the LUT values.
- Aerosol models are prescribed, which limits the number of possible aerosol properties and requires a full inversion for each different model.
- Aerosol load is assumed constant during the course of the day.

These limitations have been alleviated by Dubovik (2010) who prototyped an algorithm for the joint retrieval of surface reflectance and aerosol properties for the Meteosat Third Generation Flexible Combined Imager (MTG/FCI) with an explicit aerosol optical thickness retrieval, including diurnal variations. The inversion itself relies on an OE approach seeking the optimal balance between information that can be derived from the observations, and the one that is derived from *a priori* knowledge on the system, such as background climatological values and/or constraints on the spatial, temporal, and spectral variations of the retrieved or model state variables.

Methods based on the joint retrieval (JOI) of surface BRF and aerosol properties are therefore recommended for the estimation of PROBA-V surface reflectance. The methods proposed by Govaerts and Lattanzio (2007), Govaerts et al. (2010) or Martonchik (1997) rely on pre-defined aerosol models, which might have an impact on the retrieved surface reflectance accuracy when the wrong aerosol model is used.

### 4.4. INVERSION METHOD

#### 4.4.1. RTM SOLVING

*Most of the methods listed in Table 5 rely on LUTs to solve the forward radiative transfer model. This technique permits to speed-up the retrieval algorithm, but presents several drawbacks, in particular in case of the joint aerosol-surface BRF retrieval. In order to limit the size and dimension of the LUTs, it is necessary to bound the state variable coverage in the solution space, thereby reducing the accuracy and/or reliability of the solution. When possible, it is recommended to use a fast enough RTM, so that it can be inverted during the retrieval processed.*

#### 4.4.2. PRIOR INFORMATION (PRI)

All methods rely on prior information or assumptions, such as prescribed aerosol, or surface anisotropy (e.g., **LER**), but only a very limited number of them actually accounts for the effects of this information on the retrieved solution, *i.e.*, on the value and shape of the cost function. Those that do not include this mathematical processing are referred to as **NO**, as opposed to those relying on optimal estimation (**OE**). The goal of such an approach is to seek an optimal balance between information that can be derived from the observations, and the one that is derived from *a priori* knowledge on the system. One of the advantages of the OE approach is that it offers the possibility of a rigorous analysis of the uncertainties associated with the retrieved solution. These estimated errors should be interpreted under the assumption that the forward model behaves linearly in the vicinity of the solution and that it actually represents the observed medium, *i.e.*, a reasonably plane-parallel atmosphere in nature. Additionally, Govaerts et al. (2010) proposed a way to convert assumptions into an equivalent radiometric error and propagate this error into the estimated retrieval uncertainties. Retrieval algorithms based on Optimal Estimation techniques (Rodgers 2000; Tarantola 1998; Dubovik et al. 2011) are therefore recommended.

#### **4.4.3. MULTI-DIMENSIONAL RETRIEVAL (DIM)**

Simultaneous inversion of a large group of pixels within one or several images allows taking advantage from known limitations on spatial, spectral, and temporal variability in both aerosol and surface properties. In the method proposed by Dubovik et al. (2011), pixel-to-pixel and/or day-to-day variations of the retrieved parameters are forced to be smoothed by an additional appropriate set of *a priori* constraints. This concept is aimed to achieve a higher retrieval consistency, because in such an approach the solution over each single pixel is benefiting from information contained in co-incident observations over neighbouring pixels, as well as from land surface reflectance information obtained in preceding and subsequent observations over the same pixels. A multi-dimensional approach, which at least includes the angular one, is therefore highly recommended for the surface BRF retrieval.

#### **4.5. DISCUSSION**

This Chapter reviewed the methods listed in Table 5 according to the criteria established in Table 4 to determine the most appropriate method for the PROBA-V surface reflectance retrieval. The analysis suggests using a physically-based joint surface-aerosol retrieval approach relying on an OE inversion technique. This type of approach has proven to be very robust and has been implemented at EUMETSAT, JMA, and NOAA for the systematic processing of archived geostationary observations for the retrieval of surface reflectance from any archived geostationary observation. It relies on a reduced number of assumptions that can be easily modified to find the best balance between processing speed and accuracy.

The proposed method relies on an accumulation of PROBA-V observations forming a multi-angular and multi-spectral observation vector. While the surface properties are assumed temporally invariant during this accumulation period, the aerosol concentration will be retrieved for each clear-sky processed image.

The forward model that will be used for the retrieval solves the radiative transfer online and does not rely on LUTs anymore to the exception of the gaseous transmittance in Proba-V spectral bands.



## CHAPTER 5    ATMOSPHERIC CORRECTION VALIDATION

---

### 5.1. AEROSOL OPTICAL THICKNESS AND ATMOSPHERIC CORRECTION VALIDATION

Validation of the proposed methodology will be performed in two parts: (1) validation of the retrieved AOT and (2) an implicit validation of the total atmospheric correction through validating the TOC reflectance. Although both parts can be validated with both *in-situ* surface and satellite-based observations, focus will be on the former and latter for the validation of AOT and surface reflectance, respectively. The motivation for this will be elaborated on later in this Chapter.

First, various validation efforts on AOT and surface reflectance that were reported in scientific papers will be discussed. Second, we will highlight some common issues that come into play when comparing satellite with surface observations, including some recent efforts to address these issues. Finally, a short description of the validation set-up will be given.

### 5.2. STATE-OF-THE-ART ON ATMOSPHERIC CORRECTION VALIDATION

#### 5.2.1. AOT RETRIEVAL VALIDATION

The retrieved AOT from the proposed Optimal Estimation method is representative for 0.55  $\mu\text{m}$  and will be compared with surface observations performed at about 100 selected AERONET stations (Holben et al., 1998). At these stations, various radiation-related quantities, among which the aerosol optical thickness and Angström parameter, are derived using uniform instrumentation and calibration. The aerosol optical thickness is derived at 0.44 and 0.67  $\mu\text{m}$ , which implies that direct comparison of the retrieved AOT at 0.55  $\mu\text{m}$  with AERONET would not be possible. However, the AOT at 0.55  $\mu\text{m}$  can be interpolated using the values measured at 0.44 and 0.67  $\mu\text{m}$  and the Angström parameter as follows:

$$\tau_{\lambda} = \tau_{\lambda_0} \left( \frac{\lambda}{\lambda_0} \right)^{-\alpha}$$

with  $\lambda$  and  $\lambda_0$  being 0.55  $\mu\text{m}$  and 0.44  $\mu\text{m}$ , respectively.

AOT is retrieved from numerous satellite platforms and has been widely validated. Satellite-derived AOT has been/is retrieved from among others polar orbiting satellite instruments such as MODIS, MISR, the Polarization and Directionality of the Earth's Reflectance (POLDER), the Cloud-Aerosol Lidar with Orthogonal Polarization (CALIOP), the SCanning Imaging Absorption Spectrometer for Atmospheric Chartography (SCIAMACHY), and the Ozone Monitoring Instrument (OMI). More recently, also observations from geosynchronous satellites, such as the Geostationary Observational Environmental Satellite (GOES) and Meteosat-SEVIRI were used to retrieve AOT.

Most satellite AOT retrieval algorithms utilise the visible and near-infrared spectral range. However, satellite missions that are more dedicated to quantifying the climate forcing resulting

from (anthropogenic) emissions focus more on using specific absorption bands in ultra violet spectral channels.

A large inter-comparison of ten satellite aerosol retrieval algorithms from six satellite platforms with *in-situ* observations over European AERONET sites was performed by Kokhanovsky et al. (2007). They showed that spatial averages of the algorithm results compared well, but pixel-by-pixel differences, as well as differences in the obtained frequency distributions, were substantial. In addition, both large under- and overestimations for some algorithms compared to the AERONET observations were found. Aerosol optical thickness retrievals from the MODIS and MISR instruments have been frequently validated. Chu et al. (2002) compared MODIS AOT retrievals with AERONET measurements on four continents and found a very good comparison for inland regions ( $RMSE \leq 0.1$ ). Tripathi et al. (2005) found a low difference ( $0.12 \pm 0.11$ ) between MODIS and AERONET AOT over India during the non-dust season, which increased with increasing dust abundance ( $0.40 \pm 0.20$ ). In contrast, Schaap et al. (2008) found a large and season-dependent positive bias of MODIS AOT comparisons with AERONET over Europe of up to 50%. They argued that this large bias could be due to non-detected thin clouds that contaminate the MODIS retrievals.

Validation of the multi-angle MISR AOT retrievals was done over desert areas by Martonchik et al. (2004). It was shown that despite the infrequent measurements, the temporal evolution of aerosols could be well followed, with a retrieval uncertainty of about 0.08 at the instrument's nominal resolution. Kahn et al. (2005) performed a global 2-yr comparison of MISR and AERONET AOT and found very good agreement ( $r > 0.7$ ). Similar high correlation coefficients were found for MISR and AERONET comparisons over the Beijing metropolitan area by Jiang et al. (2007).

More recently, substantial efforts were taken to retrieve AOT information from geosynchronous satellite measurements. Bernard et al. (2011) use differences between simulated and observed SEVIRI 0.63  $\mu\text{m}$  and 1.6  $\mu\text{m}$  observations, combined with aerosol modelling, to retrieve the AOT. They showed that the relative AOT error between SEVIRI and AERONET decreases from 63% for  $AOT < 0.1$  to  $< 1\%$  for  $AOT \geq 0.3$ . Further, it was demonstrated that the retrieved temporal AOT signal correlates well with the surface observations. Daily AOT from the joint-aerosol surface reflectance technique of Govaerts et al. (2010) applied to SEVIRI measurements showed good agreement with both AERONET and MODIS AOT (Wagner et al., 2010).

### 5.2.2. SURFACE REFLECTANCE VALIDATION

The validation of surface reflectance retrievals with ground-based *in-situ* observations is somewhat more complicated than that of aerosol optical thickness:

- The *in-situ* surface reflectance spatial representativeness is dependent on the heterogeneity of the underlying surface
- A dependency of albedometer/pyranometer measurements with height above surface
- Different spectral sensitivities between satellite and ground-based observations; the surface instruments designed to measure surface albedo are sensitive over the entire solar spectrum, in contrast to the narrow PROBA-V bands.

Several surface reflectance comparison studies were performed between two or more satellite platforms. Koelemeijer et al. (2003) constructed a global surface reflectance database from the Global Ozone Monitoring Experiment (GOME) observations in the UV and VIS range, which showed good agreement with corresponding Total Ozone Mapping Spectrometer (TOMS) surface reflectance observations. A global intercomparison of MISR and MODIS surface albedos by Pinty et al. (2011) revealed that MISR overestimates relative to MODIS and that this can be partly attributed to weaker seasonal changes observed by MODIS poleward from the equator. Another

global comparison of annual mean MODIS surface albedo retrievals with ground observations at 53 FLUXNET stations by Cescatti et al. (2012) showed a very high correlation ( $r = 0.82$ ). However, it was stressed that the validation was sensitive to including only FLUXNET sites that fulfilled strict land surface homogeneity criteria. Other approaches to circumvent the sensitivity of validation results to land surface heterogeneity were carried out by e.g. Roman et al. (2009) and Liang et al. (2002). Liang et al. (2003) performed comparisons of narrow- to broad-band converted surface albedos for a number of sensors with surface observations in the US and proved that the accuracy was sufficient for land surface modelling.

Alternatively, the combination of TOA reflectances with ground-based aerosol and water vapour measurements can be used to arrive at simulated TOC reflectances. These reflectances are then compared with retrieved TOC reflectances, in order to assess the impact of any incorrect aerosol and water vapour modelling in the total atmospheric correction and to characterise the impact of the temporal variation of aerosol properties to the retrieved TOC reflectance. An example of such an exercise can be found in Vermote and Saleous (2006).

### **5.3. COMPARISON OF SATELLITE WITH GROUND-BASED OBSERVATIONS**

Comparing satellite retrievals with ground-based observations can be considerably hampered by various factors. First, one needs to take into account the differences in spatial representativeness between the satellite and surface retrievals. In PV-LAC, PROBA-V AOT and TOC reflectance retrievals from the proposed methodology represent a spatial average over  $1 \text{ km}^2$ , while surface observations typically represent spatial averages in the order of tens to hundreds of meters, depending on among others the field of view of the surface instrument (sunphotometer, pyranometer or albedometer), the surface heterogeneity, and the aerosol layer height.

An often used approach in comparing satellite retrievals to surface measurements is to simply apply temporal averaging of the surface measurements centered at the satellite observation time and to average the satellite retrievals in a square box around the station's geolocation. Such an approach implicitly assumes application of an average wind speed, that turbulent processes are virtually absent (Taylor's hypothesis of frozen turbulence), and the directionality of the advection is neglected.

Ideally, one should take the direction and speed of an advected aerosol field over the surface reference site into account to optimise the satellite to surface comparison. Such issues were reported and tackled in various other atmospheric research fields, such as in the validation of satellite cloud properties [e.g. Roca et al. (2010), Greuell and Roebeling (2009), and Schutgens and Roebeling (2009)] and satellite surface reflectance and transmittance retrievals (e.g. Deneke et al., 2009). The latter investigated the temporal variance of satellite- and ground-observed atmospheric reflectance and transmittance at different temporal scales using wavelet analysis and proposed a temporal averaging interval for ground measurements of 40 – 80 minutes to evaluate instantaneous retrievals from polar satellites over areas with sizes of  $\sim 60 \times 60 \text{ km}^2$ . Another complicating factor in the satellite to surface comparison is the land surface heterogeneity. To match the sub-pixel variability with the area-averaged satellite observations, Roman et al. (2009) and Cescatti et al. (2012) used geostatistical techniques (semi-variograms) to characterise the land surface heterogeneity, which were subsequently used to optimise the satellite versus surface comparison.

### **5.4. VALIDATION APPROACH**

The direct AOT and TOC reflectance retrieval validation, i.e., comparison with ‘ground truth’ reference observations, is currently being performed within other projects and is thus not a PV-LAC project objective. However, a comparison of the current AOT and TOC reflectance retrievals with corresponding retrievals from the OE method is part of the PV-LAC validation.

### 5.4.1. AEROSOL OPTICAL THICKNESS VALIDATION

The validation of the OE AOT will be carried out through comparison of the retrieved single-pixel value centered at the 93 selected AERONET and 7 Committee of Earth Observation Satellites (CEOS) Pseudo Invariant Calibration Sites (PICS) with ground-based observed AOT at these sites. See Figure 3 for the global distribution of these sites.

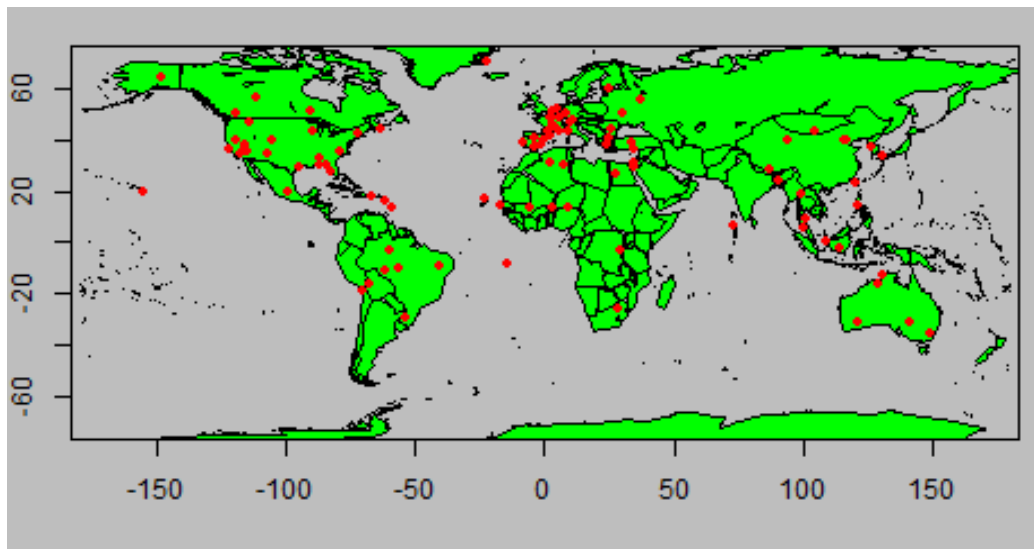


Figure 3: Global distribution of selected AERONET and CEOS PICS sites.

To arrive at a proper surface to ground comparison, several techniques were highlighted in Chapter 5.3. However, within the framework of PV-LAC a full implementation of any of these techniques would require a too large effort. In addition, the proposed Optimal Estimation method will only be used to retrieve AOT and TOC reflectance for a single pixel. Therefore we will validate the single-pixel AOT with ground-based AOT averaged over 5 minutes. .

### 5.4.2. TOC REFLECTANCE VALIDATION

Validation of the derived TOC reflectance is less straightforward to perform using *in-situ* observations, due to the intrinsic differences in the observed quantities. These differences boil down to spectral response and spatial representativeness differences, as discussed in Chapter 5.2.2. Therefore we opt for validation with other satellite surface reflectance datasets to get a first indication on the algorithm’s quality.

An additional project goal of PV-LAC is to perform an intercomparison between the current operational atmospheric correction (see CHAPTER 3) and the OE method. This quality assessment will be obtained indirectly, i.e., through comparison of the current TOC reflectances with the OE-

retrieved ones. A direct comparison of the current operational method with reference data (AERONET and MODIS MCD43A3) will be done within other projects.

The TOC reflectances for the subsets centered at the ground reference sites will be compared with spatially and temporally collocated surface reflectances from the MODIS MCD43A3 Collection 6 product. The MODIS surface albedo product is a composite of Terra and Aqua observations collected over 16 days and is provided at 500 m resolution for MODIS Bands 1 – 7 (0.62 – 2.16  $\mu\text{m}$ ). The MCD43A3 data include both black-sky and white-sky albedo. The reported accuracy of the MCD43 albedo products is generally well within 5% for solar zenith angles  $< 70^\circ$ . To avoid geolocation inaccuracies giving noise in the validation, the single-pixel OE TOC reflectance value will be compared with  $3 \times 3$  MODIS 500 m albedo values. As for the AOT validation, the validation will focus on the time series evolution in comparison with the selected MODIS surface reflectance retrievals, as well as on the statistical consistency of the AOT and TOC reflectance datasets.

In order to characterise the sensitivity of the retrieved TOC reflectances to atmospheric parameters, such as aerosol and water vapour load, TOC reflectances simulated with PROBA-V TOA reflectance and AERONET/CEOS PICS AOT and water vapour will be compared with retrieved TOC reflectances over these AERONET/CEOS PICS sites.

#### 5.4.3. VALIDATION METRICS

As the AOT and TOC reflectances are only delivered as single-pixel values, the main aim of the AOT validation is the comparison of the obtained time series. From this time series comparison, some general statistics are derived, following the metrics proposed by Claverie et al. (2015):

- Accuracy ( $A$ )

$$A = \frac{1}{n} \sum_{i=1}^n \varepsilon_i$$

- Precision ( $P$ )

$$P = \sqrt{\frac{1}{n-1} \sum_{i=1}^n (\varepsilon_i - A)^2}$$

- Uncertainty ( $U$ )

$$U = \sqrt{\frac{1}{n} \sum_{i=1}^n \varepsilon_i^2}$$

- Relative uncertainty ( $rU$ )

$$rU = \frac{U}{\bar{m}}$$

In these equations,  $n$  is the number of valid samples used in the comparison,  $\varepsilon_i$  is the retrieved minus the reference value, and  $\bar{m}$  denotes the average of the reference observations.

Validation results will be presented for all stations, as well as stratified in categories, based on e.g. latitudinal regions, land cover, and viewing geometries.

## LITERATURE

- Anderson, G. P., Clough, S. A., Kneizys, F. X., Chetwynd, J. H., & Shettle, E. P. (1986). *AFGL atmospheric constituent profiles (0 – 120 km)* (No. AFGL-TR-86-0110). Aif Force Geophysics Lab Hanscom AFB, MA.
- Bernard, E., C. Moulin, D. Ramon, D. Jolivet, J. Riedi, and J.-M. Nicolas. 2011. "Description and Validation of an AOT Product over Land at the 0.6 Mm Channel of the SEVIRI Sensor Onboard MSG." *Atmos. Meas. Tech.* 4 (11) (November 25): 2543–2565. doi:10.5194/amt-4-2543-2011.
- Berthelot, B. and G. Dedieu, 1997, Correction of atmospheric effects for VEGETATION data. *Physical Measurements and Signatures in remote sensing*, p.19-25
- Cescatti, A., and Coauthors. (2012). Intercomparison of MODIS albedo retrievals and in situ measurements across the global FLUXNET network. *Remote sens. Environ.*, 121, 323-334.
- Chu, D. A., Kaufman, Y. J., Ichoku, C., Remer, L. A., Tanré, D., and Holben, B. N. (2002). Validation of MODIS aerosol optical depth retrieval over land. *Geophys. Res. Lett.*, 29(12).
- Claverie, M., Vermote, E. F., Franch, B., & Masek, J. G. (2015). Evaluation of the Landsat-5 TM and Landsat-7 ETM+ surface reflectance products. *Remote Sens. Environ.*, 169, 390-403.
- Deneke, H. M., Knap, W. H., and Simmer, C. (2009). Multiresolution analysis of the temporal variance and correlation of transmittance and reflectance of an atmospheric column. *J. Geophys. Res.*, 114(D17).
- Dubovik, O. 2010. *Study on Improved Retrieval Method Of Detailed Aerosol Properties from MTG/FCI, Part 1, Theoretical Concept*. EUMETSAT ITT No 09/992.
- Dubovik, O., M. Herman, A. Holdak, T. Lapyonok, D. Tanré, J. L. Deuzé, F. Ducos, A. Sinyuk, and A. Lopatin. 2011. "Statistically Optimized Inversion Algorithm for Enhanced Retrieval of Aerosol Properties from Spectral Multi-angle Polarimetric Satellite Observations." *Atmos.Meas.Tech.* 4: 975–1018.
- Geiger, B., D. Carrer, L. Franchisteguy, J.-L. Roujean, and C. Meurey. 2008. "Land Surface Albedo Derived on a Daily Basis From Meteosat Second Generation Observations." *IEEE Transact. Geosci. Remote Sens.*, 46 (11) (November): 3841 –3856. doi:10.1109/TGRS.2008.2001798.
- Gobron, N., B. Pinty, M. M. Verstraete, and Y. M. Govaerts. "A Semi-discrete Model for the Scattering of Light by Vegetation." *J. Geophys. Res.*, 102 (1996): 9431 – 9446.
- Govaerts, Y., and A. Lattanzio. 2007. "Retrieval Error Estimation of Surface Albedo Derived from Geostationary Large Band Satellite Observations: Application to Meteosat-2 and -7 Data." *J. Geophys. Res.*, 112 (D05102): doi:10.1029/2006JD007313.
- Govaerts, Y., A. Lattanzio, M. Taberner, and B. Pinty. 2008. "Generating Global Surface Albedo Products from Multiple Geostationary Satellites." *Remote Sens. Environ.*: doi:10.1016/j.rse.2008.01.012.
- Govaerts, Y. M., S. Wagner, A. Lattanzio, and P. Watts. 2010. "Joint Retrieval of Surface Reflectance and Aerosol Optical Depth from MSG/SEVIRI Observations with an Optimal Estimation Approach: 1. Theory." *J. Geophys. Res.*, 115 (D02203) (January 1): doi:10.1029/2009JD011779.
- Herman, J. R., and E. A. Celarier. 1997. "Earth surface reflectivity climatology at 340–380 nm from TOMS data." *J. Geophys. Res.*, 102 (D23) (December 20): 28003–28,011. doi:10.1029/97JD02074.
- Jiang, X., Liu, Y., Yu, B., & Jiang, M. (2007). Comparison of MISR aerosol optical thickness with AERONET measurements in Beijing metropolitan area. *Remote Sens. Environ.*, 107(1), 45-53.

## Literature

- Jin, Y., C. B. Schaaf, F. Gao, X. Li, A. H. Strahler, W. Lucht, and S. Liang. 2003. "Consistency of MODIS Surface Bidirectional Reflectance Distribution Function and Albedo Retrievals: 1. Algorithm Performance." *J. Geophys. Res.*, 108 (D5): 4158, doi:10.1029/2002JD002803.
- Kahn, R. A., Gaitley, B. J., Martonchik, J. V., Diner, D. J., Crean, K. A., & Holben, B. (2005). Multiangle Imaging Spectroradiometer (MISR) global aerosol optical depth validation based on 2 years of coincident Aerosol Robotic Network (AERONET) observations. *J. Geophys. Res.*, 110(D10).
- Kleipool, Q. L., M. R. Dobber, J. F. de Haan, and P. F. Levelt. 2008. "Earth surface reflectance climatology from 3 years of OMI data." *J. Geophys. Res.*, 113 (D18) (September 24): D18308. doi:10.1029/2008JD010290.
- Knapp, K. R., R. Frouin, S. Kondragunta, and A. Prados. 2005. "Toward Aerosol Optical Depth Retrievals over Land from GOES Visible Radiances: Determining Surface Reflectance." *Int. J. Remote Sens.*, 26 (18): 4097–4116.
- Koelemeijer, R. B. A., J. F. de Haan, and P. Stammes. 2003. "A database of spectral surface reflectivity in the range 335–772 nm derived from 5.5 years of GOME observations." *J. Geophys. Res.*, 108 (D2) (January 30): 4070. doi:10.1029/2002JD002429.
- Kokhanovsky, A. A., Breon, F. M., Cacciari, A., Carboni, E., Diner, D., Di Nicolantonio, W., ... & Li, Z. (2007). Aerosol remote sensing over land: A comparison of satellite retrievals using different algorithms and instruments. *Atmos. Res.*, 85(3), 372-394.
- Liang, S., Shuey, C. J., Russ, A. L., Fang, H., Chen, M., Walthall, C. L., ... & Hunt, R. (2003). Narrowband to broadband conversions of land surface albedo: II. Validation. *Remote Sens. Environ.*, 84(1), 25-41.
- Liang, S., Fang, H., Chen, M., Shuey, C. J., Walthall, C., Daughtry, C., ... & Strahler, A. (2002). Validating MODIS land surface reflectance and albedo products: Methods and preliminary results. *Remote Sens. Environ.*, 83(1), 149-162.
- Lucht, W., C. B. Schaaf, and A. H. Strahler. 2000. "An Algorithm for the Retrieval of Albedo from Space Using Semiempirical BRDF Models, 38, , 2000." *IEEE Transact. Geosci. Remote*, 38: 977 - 998.
- Lyapustin, A., and coauthors, 2010. "Analysis of Snow Bidirectional Reflectance from ARCTAS Spring-2008 Campaign." *Atmos. Chem. Phys.* 10, 4359 - 4375. doi:10.5194/acp-10-4359-2010.
- Lyapustin, A. I. 1999. "Atmospheric and Geometrical Effects on Land Surface Albedo." *J. Geophys. Res.*, 104 (D4): 4127–4143.
- Maisongrande, P., Duchemin, B., Berthelot, B. D., Dubegny, C., Dedieu, G., and Leroy, M. (2001). New composite products derived from the SPOT/VEGETATION mission. In *Physical measurements & signatures in remote sensing. International symposium* (pp. 239-248).
- Martonchik, J. V., Diner, D. J., Kahn, R., Gaitley, B., & Holben, B. N. (2004). Comparison of MISR and AERONET aerosol optical depths over desert sites. *Geophys. Res. Lett.*, 31(16).
- Martonchik, J. V. 1997. "Determination of Aerosol Optical Depth and Land Surface Directional Reflectances Using Multiangle Imagery." *J. Geophys. Res.*, 102 (D14): 17014–17022.
- Pinty, B., F. Roveda, M. M. Verstraete, N. Gobron, Y. Govaerts, J. V. Martonchik, D. J. Diner, and R. A. Kahn. 2000. "Surface Albedo Retrieval from Meteosat: Part 1: Theory." *J. Geophys. Res.*, 105: 18099–18112.
- Pinty, Bernard, Malcolm Taberner, Vance R. Haemmerle, Susan R. Paradise, Eric Vermote, Michel M. Verstraete, Nadine Gobron, and Jean-Luc Widlowski. 2011. "Global-Scale Comparison of MISR and MODIS Land Surface Albedos." *J. Clim.*, 24 (3) (February): 732–749. doi:10.1175/2010JCLI3709.1.

## Literature

- Rahman, H., & Dedieu, G. (1994). SMAC: a simplified method for the atmospheric correction of satellite measurements in the solar spectrum. *Remote Sensing*, 15(1), 123-143.
- Rodgers, C. D. 2000. *Inverse Methods for Atmospheric Sounding*. Ed. F. W. Taylor. Series on Atmospheric Oceanic and Planetary Physics. World Scientific.
- Schaap, M., Timmermans, R. M. A., Koelemeijer, R. B. A., De Leeuw, G., & Builtjes, P. J. H. (2008). Evaluation of MODIS aerosol optical thickness over Europe using sun photometer observations. *Atmos. Environ.*, 42(9), 2187-2197.
- Tarantola, A. 1998. *Inverse Problem Theory : Methods for Data Fitting and Model Parameter Estimation*. Vol. 3rd edition. Elsevier.
- Tripathi, S. N., Dey, S., Chandel, A., Srivastava, S., Singh, R. P., & Holben, B. N. (2005, June). Comparison of MODIS and AERONET derived aerosol optical depth over the Ganga Basin, India. In *Ann. Geophys.* (Vol. 23, No. 4, pp. 1093-1101).
- Vermote, E. F., and A. Vermeulen. 1999. *Atmospheric Correction Algorithm: Spectral Reflectances (MOD09). Algorithm Technical Background Document (ATBD)*. [http://modis.gsfc.nasa.gov/data/atbd/atbd\\_mod08.pdf](http://modis.gsfc.nasa.gov/data/atbd/atbd_mod08.pdf).
- Vermote, E., C.O. Justice, and F.-M. Breon. 2009. "Towards a Generalized Approach for Correction of the BRDF Effect in MODIS Directional Reflectances." *IEEE T. Geosci. Remote*, 47 (3) (March): 898–908. doi:10.1109/TGRS.2008.2005977.
- Vermote, Eric F, Nazmi Z El Saleous, and Christopher O Justice. 2002. "Atmospheric Correction of MODIS Data in the Visible to Middle Infrared: First Results." *Remote Sens. Environ.*, 83 (1–2) (November): 97–111. doi:10.1016/S0034-4257(02)00089-5.
- Vermote, E. F., & Saleous, M. N. (2006). Operational atmospheric correction of MODIS visible to middle infrared land surface data in the case of an infinite Lambertian target. In *Earth Sci. Sat. Remote Sens.* (pp. 123-153). Springer Berlin Heidelberg.
- Wagner, S. C., Govaerts, Y. M., & Lattanzio, A. (2010). Joint retrieval of surface reflectance and aerosol optical depth from MSG/SEVIRI observations with an optimal estimation approach: 2. Implementation and evaluation. *J. Geophys. Res.*, 115(D2).
- Wang, Y., A. I. Lyapustin, J. L. Privette, R. B. Cook, S. K. SanthanaVannan, E. F. Vermote, and C. L. Schaaf. 2010. "Assessment of Biases in MODIS Surface Reflectance Due to Lambertian Approximation." *Remote Sens. Environ.*, 114 (11): 2791–2801.
- Zhou, Y., D. Brunner, R. J. D. Spurr, K. F. Boersma, M. Sneep, C. Popp, and B. Buchmann. 2010. "Accounting for Surface Reflectance Anisotropy in Satellite Retrievals of Tropospheric NO<sub>2</sub>." *Atmos. Meas. Tech.*, 3 (5): 1185–1203. doi:10.5194/amt-3-1185-2010.